DEVELOPING HIGH SPATIAL RESOLUTION DAYTIME CLOUD CLIMATOLOGIES FOR AFRICA

Michael Douglas[1], Rahama Beida[2], and Abdul Dominguez[2]
[1]*National Severe Storms Laboratory,* [2]*Cooperative Institute for Mesoscale Meteorological Studies and University of Oklahoma*
Norman, Oklahoma USA

Abstract

MODIS imagery has been used to develop a short-period climatology of visible cloudiness for the African continent at approximately 250 m spatial resolution. The MODIS imagery, from the NASA Terra and Aqua satellite overpasses at ~1030 and 1330 Local Time (LT) are used to produce visible cloud frequencies that provide a good estimate of mid-day cloudiness. Though only available for about 5 years, the fields reflect strong – topographic and geographical controls on the mean cloudiness. Over much of Africa these controls are independent of season and are evident in the monthly means of any year. Most patterns can be explained as a consequence of diurnally-driven circulations associated with sloping topography or land-water contrasts. Other regions with frequent cloudiness reflect the interaction of prevailing winds with topography. The cloud frequency results should be of value to African forecasters who wish to understand better their regional and local climatology.

1. Introduction

In this study, we use satellite imageries from the Moderate Resolution Imaging Spectrometer (MODIS) instruments on the NASA Terra and Aqua satellites to develop a short-period climatology of visible cloudiness for the African continent, with a special focus on the Ethiopian highland, at approximately 250 m spatial resolution. This high-resolution cloud climatology could help forecaster's improve their understanding of the smaller-spatial scale structure of the cloud climatologies in their particular regions of interest. Many other applications of such climatologies are possible, ranging from solar energy to aid in mapping biodiversity and the ranges of individual species.

2. Data and Methods

MODIS imagery were obtained from the NASA MODIS Rapid Response website (http://rapidfire.sci.gsfc.nasa.gov/subsets/). These images have approximately 250m pixel size at nadir and the navigational accuracy is excellent. The original "true-color" jpg files were converted into gray scale images and the cloudy pixels were identified by being brighter than a certain threshold. While the method used to identify cloudy pixels yields unrealistic results in areas of very high reflectivity, such as salt flats and ice fields, this problem does not affect most tropical regions where cloudiness is easily extracted from the generally darker forest or ocean background. Finally, Google Earth Pro was used to assemble the different sectors images into larger mosaics.

The individual daily cloud/no-cloud data was averaged by satellite, by month, and eventually averaged together to obtain multi-year means. These means images are updated regularly and displayed at the NSSL website:

http://www.nssl.noaa.gov/projects/pacs/web/MODIS/

Since the data being used varies with the sectors NASA makes available on its web page, some sectors have only a few year's data while others have more than six. Ideally the full raw data set would have been processed, but personnel were limited to do this.

3. The cycle of seasonal mean cloudiness

3.1 Northern Hemisphere Summer season

During the summer season defined here as the averages for the period May-October (Figs. 1a-b), cloud cover is mainly concentrated over West, Central and East Africa, within a band extending from 5°S to 10°N. This cloudiness is linked with the northward movement of the ITCZ and the associated monsoon, and the trade wind troughs. Highest percentages of cloud cover occur over the Gulf of Guinea countries, the Ethiopian Highland, Kenya, Rwanda, Burundi and the east coast of Madagascar. Cloud-cover frequency decreases northward of the maximum cloudiness band to nearly 0% over the Sahara desert.

Very low percentages of cloud cover (less than 10%) are found in the vicinity of the Sahara desert over the Sahelian regions of West Africa, that encompassed northern Senagal, Mauritania, southern Mali, Niger, Chad, and Sudan. Over the coastal regions of West Africa, a double maximum with varying intensity is evident over southern Nigeria and Guinea, associated with the Jos platau and the Fouta Djalon montains respectively. Another maximum associated with the Ethiopian highland is also evident over the eastern part of the continent.

It should be noted that the northern Hemisphere summer corresponds to the dry season over Southern Africa where little to no cloud conditions are observed, except over localized areas where orography plays an important role in the formation of local clouds (e.g. east coast of Madagascar), and the south-eastern part of

South Africa where cloudiness is associated with eastward propagating extra-tropical frontal systems. There is a maximum in low stratus clouds off the Namibian cost which is evident in both seasons (varying length of record for the different sectors makes the mosaic poor in this region).

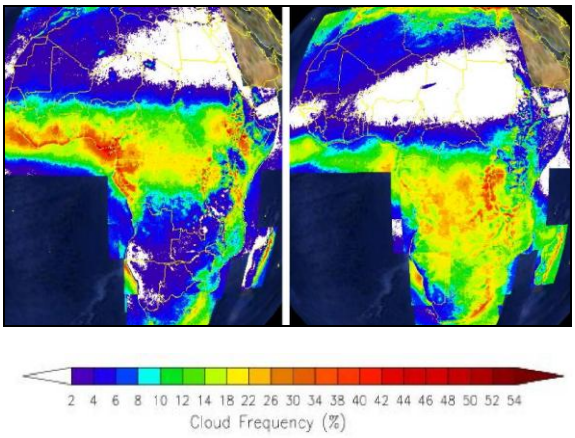

Fig. 1a. May-Oct mean cloudiness (left) and Nov-Apr (right).

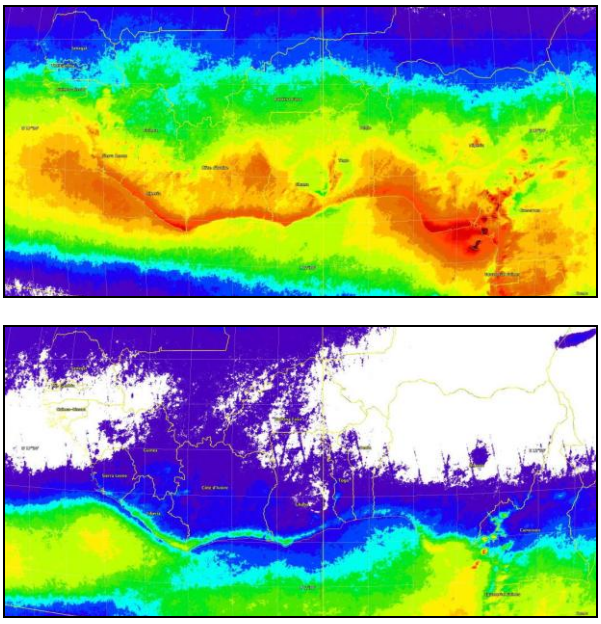

Fig. 1b. Same as Fig. 1a except a closer view of west African region.

3.2 Southern Hemisphere summer season

Cloud-cover averages derived from MODIS for the period of November-April (southern hemisphere summer season), are shown in Fig.1b. Contrary to the northern hemisphere summer, where cloudiness is located over a narrow band, significant cloud cover spreads over most of the Southern Hemisphere, with a maximum cloudiness over around the east African Rift Valley region, and the south-eastern part of South Africa .

The only pronounced minimum cloud zone in the SH is located along the west coast and is associated with the Kalahari desert. The most significant contrast in cloud cover is observed over Madagascar where the cloud cover frequency varies from 32% over the east coast to less than 8% over south central part.

Clear skies prevail over much of north Africa as a consequence of the southward retreat of the monsoon, and the prevailing sub-tropical high pressure systems over the region. The significant cloud cover observed in this area are associated with the ITCZ over the Gulf of Guinea and the cumulative effect of extra-tropical frontal systems closer to the Mediterranean. There is an interesting increase in cloud frequency over western Mali, separating two more cloud free zones. This is also evident during the summer season as well.

4. Mesoscale features associated with diurnal circulations.

Although some parts of Africa are relatively free of detailed cloudiness variations, there are many parts that show large spatial gradients. The Ethiopian highlands is one such area (Fig. 2). To the west of the highland area (over Chad) the spatial variations of cloudiness are gradual and the strong seasonality is evident. In the highly irregular topography of Ethiopia the cloud maxima and minima are strongly correlated with relatively high and low terrain respectively. Cloudiness is a minimum in broad valleys, associated with the descending branch of the valley breezes. Conversely, surrounding high terrain shows maximum values. And although the cloud amounts are much less in Nov-Apr, the same max and min patterns are found associated with the topography.

Although there should be a general relationship between cloudiness and rainfall in the moist tropics, it is not easy to directly relate the MODIS-estimates cloudiness patterns to rainfall. Late afternoon and evening storms will be missed by the Terra and Aqua overpasses. It should be remembered that the results shown here show cloud frequency, not rainfall patterns, though in some regions the spatial patterns can be very similar.

The importance of slope- and land-water contrasts is evident in fig. 3, which shows the difference in cloudiness between the 1330LT and 1030LT cloud frequencies. Cloudiness decreases (red shades) over the large lakes of central east Africa as the day progresses, while cloudiness increases (blue shades) over the surrounding higher terrain. Lake Victoria is the most obvious features, but most of the rift valley lakes

show similar tendencies – though the details vary. Forecasting such geographical variations of cloudiness should be feasible on a daily basis if such climatological patterns are one component in the forecast procedure.

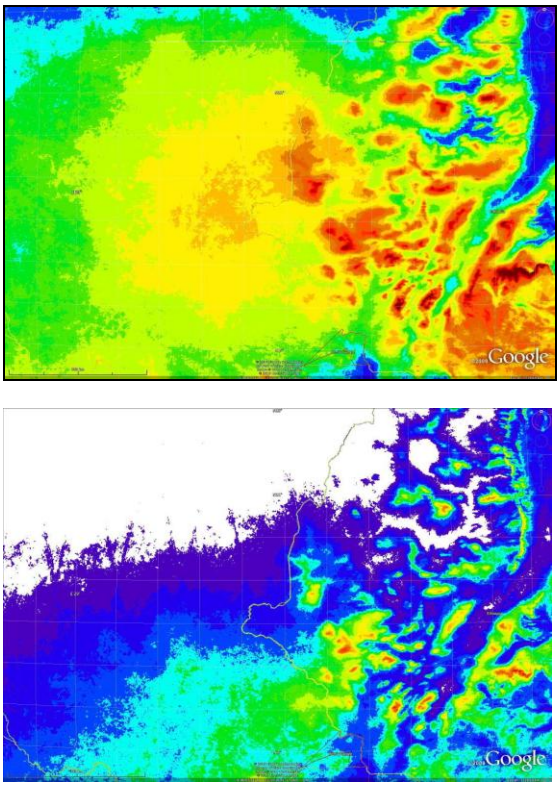

Fig. 2. May-Oct mean cloud frequency (top) and Nov-April cloudiness (bottom).

Sea-land breezes have the same impact, and are most obvious over west Africa (Fig. 4). The increase in clouds associated with the ascent of the sea-breeze front is obvious, and is most enhances where the coastline is concave, enhancing inland convergence. The decrease of cloudiness over a wide area inland from the coast and in a narrow band just offshore are also apparent; this is more evident from Fig. 5.

Fig. 5. Closer view of the region of Ivory Coast – Ghana, showing greater detail of Fig. 4. (right)

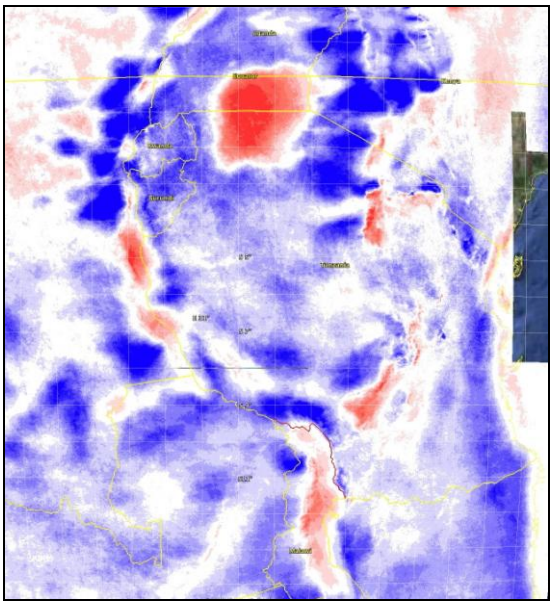

Fig. 3. Difference in cloudiness between Aqua and Terra cloudiness averaged over entire year, 5-year mean. Redder color is greater decrease during day (18% is saturated red), bluer is greater increase during day.

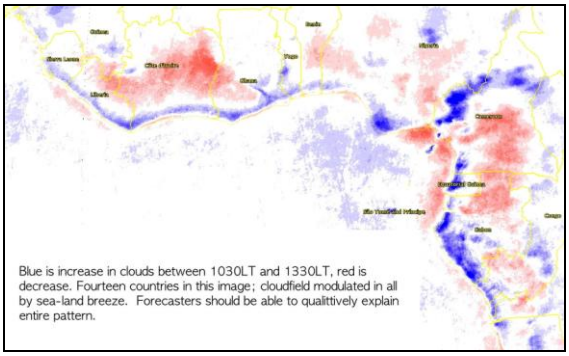

Fig. 4. Same as Fig. 3, except for West African coast area.

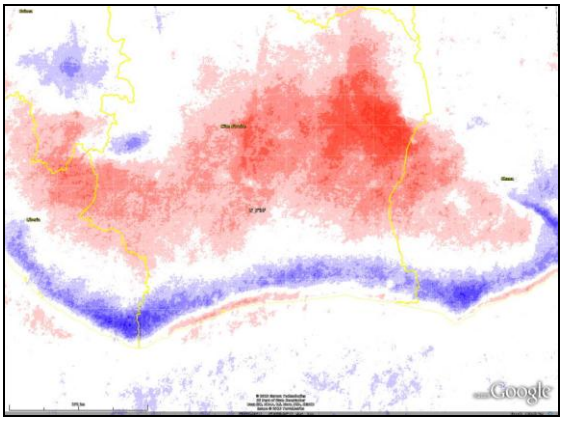

Overall, the higher-resolution of the MODIS composites can be used for a variety of meteorological or other applications. Putting the results in kmz (Google Earth) format allows for easy comparison of the mean cloudiness with the underlying surface features. One example of this, with a number of possible applications, is showing the mean cloudiness around Ngorongoro Crater in Tanzania. Enormous numbers of tourists visit this location; predicting the mean cloudiness for a cloud-free itinerary (at least based on climatology) becomes straightforward (Fig. 6).

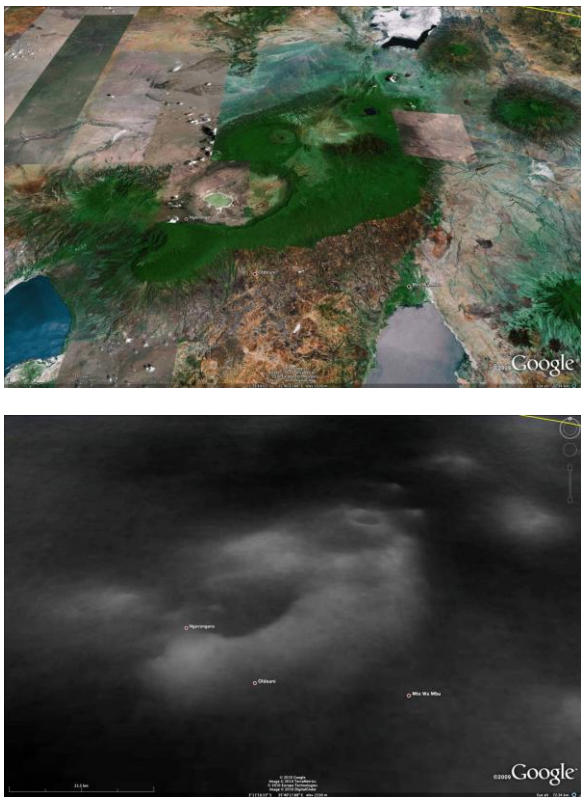

Fig. 6. Google Earth oblique perspective of Ngorongoro crater region and cloudiness (below). Gray scale shows more subtle details than color scale. Note the crater lips with enhanced cloudiness (darker=less clouds).

Acknowledgments: The NASA site: http://rapidfire.sci.gsfc.nasa.gov/subsets/ provided the data used in this study and the staff overseeing the site are thanked for permitting voluminous downloads from the site. John Mejia and Raquel Orozco developed most of the procedures used in this study.